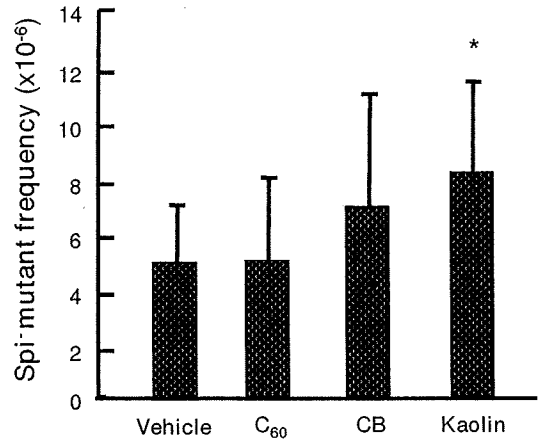

Figure 6
MFs of deletions in the lungs of *gpt* delta mice exposed to multiple doses of particles. An asterisk (*) denotes $p < 0.05$ in a Student's *t*-test of MFs of particle-treated vs. the corresponding vehicle-control mice.

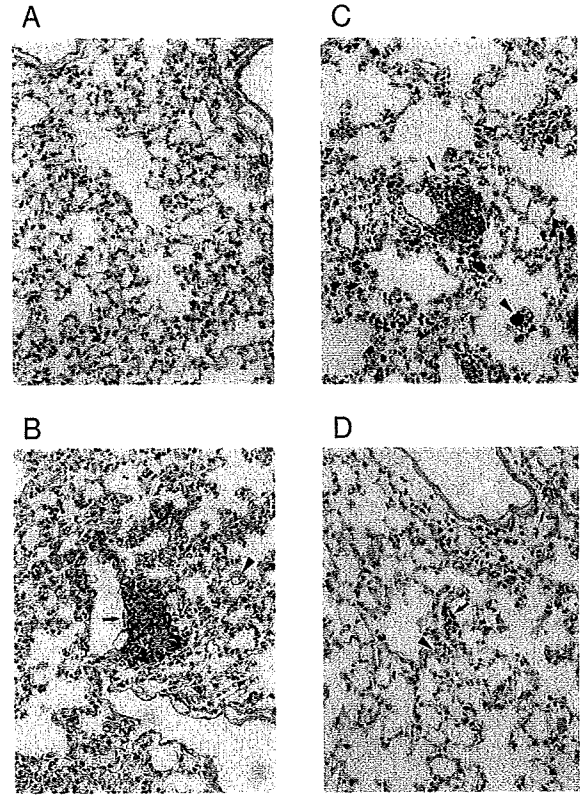

Figure 7
Microscopic findings in lungs of *gpt* delta mice intratracheally instilled with particles. Normal appearance of pulmonary parenchyma in a vehicle-control (Panel A). Pulmonary parenchyma obtained from *gpt* delta mice intratracheally instilled with four consecutive doses of 0.2 mg/mice of C_{60} (Panel B), CB (Panel C) and kaolin (Panel D). Test substance-phagocytized macrophages (arrowheads) can be observed, and granulomaous (arrows) formations are also found in lungs of particle-instilled mice. A-D; Original magnification × 40.

kinds of mutations might be same. In general, the G:C to C:G transversion is thought to be a rare event in both spontaneous and chemically-induced mutations. However, various oxidative stresses caused by sunlight, UV radiation, hydrogen peroxide and peroxy radicals frequently induce G:C to C:G transversion in *in vitro* assay systems [26-29]. Reactive oxygen species (ROS) and DNA damage, including 8-oxo-7,8-dihydro-2'-deoxyguanosine (8-oxo-dG), were reported to be increased by nanoparticles, including asbestos, treatment [4,21,30-34]. The mechanism of the generation of ROS by nanoparticles is still unclear; however, these nanoparticles would be able to trigger ROS production by iron-catalysed Fenton reactions, or would be accumulated in the cells by phagocytosis, then enhance the production of ROS from macrophages and leucocytes [35,36]. In the present study, test substance-phagocytized macrophages and granulomas were frequently observed in the lungs, and the degree of the granulomas formation was partly associated with the mutagenic effect on *gpt* gene by particles. In the case of C_{60}, generation of ROS along with lipid peroxidation via electron transfer between C_{60} and other molecules has been reported [21]. The most typical lesion of oxidative damage is 8-oxo-dG which can pair with dA and leads G to T transversions [37,38] but it is not responsible for G to C transversion since dG is not incorporated opposite 8-oxodG [37,39]. Moreover, a variety of oxidative lesion products of guanine other than 8-oxodG, including imidazolone (Iz), oxazolone (Oz), spiroiminodihydantoin (Sp) and guanidinohydantoin (Gh), have been reported [39-45]. Recently, three such molecules, Oz, Sp and Gh are thought to be the key molecules causing G to C transversion using the translesion synthesis systems [43-46]. Moreover, these molecules have also been detected in bacterial cells and rat liver [47,48]. Therefore, it is suggested that G:C to C:G transversions induced by particles such as C_{60}, CB and kaolin could involve Oz, Sp and Gh formations.

In the present study, G:C to A:T transition and A:T to T:A transversion were also increased in the particle treatment. G to A transition has commonly been observed in spontaneous and chemically-induced mutants and deamination of 5-methylcytosine or alkylation of guanine might be

involved in these mutations. In contrast to G to A transition, A:T to T:A transversion is known as a rare mutation. It has been reported that the most common mutations induced by N-ethyl-N-nitrosourea in the mouse are A:T to T:A transversions [49]. However, at present, the mechanisms underlying generation of A to T transversion by particles are still unclear.

As mentioned above, we found that all three particles, C_{60}, CB and kaolin increased significant DNA damage in the lungs compared to the vehicle control using the comet assay. Comet assay under alkaline conditions is used to detect both strand breaks and DNA altering lesions such as an AP site [50]. Moreover, in the present study, treatments with C_{60}, CB and kaolin significantly increased the frequency of micronucleated A549 cells in a dose-dependent manner. However, these genotoxic/clastogenic potencies did not necessarily correspond to the mutagenicity observed in *gpt* transgenic mice.

In conclusion, we demonstrated that manufactured nano/microparticles such as C_{60}, CB and kaolin were shown to be genotoxic in both *in vitro* and *in vivo* assay systems. Moreover, it was not necessarily the case that genotoxic potency was related to particle size (C_{60} and CB are nano-sized, but kaolin is micro-sized particles used in the present study.). From the prominent mutation spectra, it is suggested that oxidative DNA damage might be commonly involved in their mutagenicity. The dose of particles used in the present study seems to be extremely high compared with human exposure in the work place. However, it is likely that these materials would be deposited for a long time in tissues, same as those of asbestos fiber. Therefore, further studies of the mechanisms of genotoxicity and application routes other than trachea are needed. Moreover, exposure levels of these genotoxic particles in the working environment should be determined.

Materials and methods

Materials and chemicals

CB nanoparticles with a primary particle size of 14 nm (Printex 90) were obtained from Degussa, Dusseldorf, Germany. The surface area was 300 m^2/g (disclosed by Degussa). The CB was autoclaved at 250°C for 2 h before use. High purity (99.9%) C_{60} was purchased from Sigma-Aldrich. (St. Louis, MO, USA). The declared primary particle size of C_{60} was 0.7 nm. Kaolin, white crystal, with a primary particle size of 4.8 μm was obtained from Engelhard Corp., Iselin, NJ. C_{60}, CB and kaolin particles were suspended in saline (Otsuka Pharmaceutical Co. Ltd., Tokyo, Japan) containing 0.05% of Tween 80 (Nacalai Tesque, Kyoto, Japan) by sonication for 15 - 20 min, at a concentration of 2 mg/mL. The size distributions of the presently used nano/microparticles in the suspensions were measured by dynamic light scattering (DLS) using FPAR-1000 (Otsuka electronics Co., Ltd., Osaka), and the agglomeration state was assessed by transmission electron microscope (TEM) (H-7000, Hitach, Ltd., Tokyo, Japan). The size distributions were determined with the algorithm CONTIN. For the TEM assessment, an aliquot of 5 μL was put on the nickel glid coated by hydrophilized formbar and assessed with an accelerating voltage of 75 kV.

Type I agarose, low melting point agarose, dimethylsulfoxide and Triton X-100 were bought from Sigma-Aldrich. Ethidium bromide was obtained from Merck (Darmstadt, Germany). Other chemicals were purchased from Wako Pure Chemical Industries (Osaka, Japan).

Micronucleus test

Human lung carcinoma A549 cells obtained from the RIKEN Cell Bank (Wako, Japan) were cultured in Eagle's minimum essential medium (Nissui Pharmaceutical Co. Ltd., Tokyo, Japan) supplemented with 10% fetal bovine serum (JRH Biosciences, Lenexa, KS, USA) in a 5% CO_2 atmosphere at 37°C. The cells (7×10^5 cells/dish) were seeded in plastic cell culture dishes (ϕ60 mm) one day before treatment. Particles were suspended in physiological saline containing 0.05% (v/v) Tween-80 with sonication (for 5-10 min at room temperature). One volume of the suspension was mixed with 9 volumes of the culture medium with serum (altogether 3.3 mL/dish), and then cells were treated at indicated concentrations for 6 hr. Since a long exposure (48 hr) increased the frequency of micronucleated cells in the solvent control (data not shown), we chose a 6 hr treatment. After treatment, cells were further cultured for 42 hr. Then, cells were trypsinized and counted, and centrifuged. Growth inhibition was calculated by following the formula:

$$\text{Growth rate} = (\text{the number of treated cells}) / (\text{the number of non-treated cells})$$

Cells were resuspended in 0.075 M KCl, and incubated for 5 min. Cells were then fixed 4 times in methanol:glacial acetic acid (3:1), and washed with methanol containing 1% acetic acid. Finally, cells were resuspended in methanol containing 1% acetic acid. The cell solution was dropped onto slides and the nucleus was stained by mounting with 40 μg/mL acridine orange (Nacalai Tesque) solution and immediately observed by fluorescence microscopy using blue excitation. The number of cells with micronuclei was recorded based on observation of 1,000 interphase cells. The data of EMS and mitomycine C (MMC) for positive system controls in CHL cells under the same experimental conditions were as follows; Percentage of micronucleated cells were 9.8 ± 0.68 for EMS (1 mg/mL) and 10.3 ± 1.1 for MMC (100 n/mL), respectively.

Animals

Male C57BL/6J mice (9 weeks old) were purchased from Charles River Japan, Inc. (Atsugi, Japan) and *gpt* delta mice (9 weeks old) were obtained from Japan SLC (Shi-

zuoka, Japan), respectively. The *gpt* delta mice carry approximately 80 copies of *lambda* EG10 DNA on each chromosome 17 on a C57BL/6J background [23]. Animals were provided with food (CE-2 pellet diet, CLEA Japan, Inc., Tokyo, Japan) and tap water *ad libitum* and quarantined for one week. Mice were maintained under controlled conditions: 12-h light/dark cycle, 22 ± 2°C room temperature, and 55 ± 10% relative humidity. The experiments were conducted according to the "Guidelines for Animal Experiments in the National Cancer Center" of the Committee for Ethics of Animal Experimentation of the National Cancer Center.

Treatment of wild type and gpt *delta transgenic mice with particles*

All particles were well sonicated and suspended in saline containing 0.05% of Tween 80. For comet assay, 5 male C57BL/6J mice were intratracheally instilled with particles using a polyethylene tube under anesthesia with 4% halothane (Takeda Chemical, Osaka, Japan). Single doses of 0.05 or 0.2 mg per animal were employed. The control mice (n = 5) were instilled intratracheally with 0.1 mL of the solvent alone. The mice were sacrificed 3 hr after these particle administrations, and lungs were removed then used for comet assay immediately. In addition, different exposure time (24 hr) was also examined. For histological and mutation analysis, each group of 10 male *gpt* delta mice was intratracheally instilled with particles at a single dose of 0.2 mg per animal, and multiple doses of 0.2 mg per animal per week for 4 consecutive instillations, as described for comet assay. The intratracheal instillation dose of particles between 0.05 and 1 mg/mouse has been commonly used for the pulmonary inflammation and genotoxicity test [51,52]. The control mice (n = 10) were instilled intratracheally with the solvent alone. The mice were sacrificed at 22 weeks.old being 12 (for single instillation) or 8 (for multiple instillations) weeks after particle administrations, respectively. Tissues, including lungs and kidneys, were removed. Lungs and kidneys obtained from 4 mice were used for histological evaluation and examined under a light microscope for any abnormalities. For histopathological evaluation, organs were fixed in 10% neutral buffered formalin, embedded in paraffin blocks and routinely processed to H&E stained sections. The remaining 6 mice were used for mutation analysis and the tissues were stored at -80°C until the DNA was isolated.

Alkaline comet assay

The alkaline comet assay was performed according to the method of Sasaki et al. [53] or Toyoizumi et al. [54] with some modification. The lungs were taken from treated mice and weighed, and lung tissue was minced and suspended with chilled homogenizing buffer, then homogenized gently using a Dounce-type homogenizer in ice. Lung cell suspension was mixed with the same volume of 1.4% low melting point agarose in PBS. The mixture was layered on the slide coated with 0.7% agarose layer, and then covered with 0.7% low melting point agarose. After slide preparation, slides were immersed in lysing solution and refrigerated at 4°C for 1 h. Each slide was then placed in alkaline electrophoresis buffer for 10 min to allow for DNA unwinding. Electrophoresis was performed at 25 V, 300 mA for 15 min at 0°C. The slides were neutralized with Tris buffer for 5 min twice, and dehydrated with 70% ethanol to fix. The cells were stained with ethidium bromide solution. Comet images were analyzed using a fluorescence microscope (magnification 200×) equipped with a CCD camera. Fifty cells were examined per mouse. The tail moment of DNA was measured using Comet Analyzer Youworks Bio Imaging Software.

gpt and Spi⁻ mutation assays

High-molecular-weight genomic DNA was extracted from the lungs and kidneys using a RecoverEase DNA Isolation Kit (Stratagene, La Jolla, CA) according to the instruction manual provided by the supplier. *Lambda* EG10 phages were rescued using Transpack Packaging Extract (Stratagene).

The *gpt* mutagenesis assay was performed according to previously described methods [55]. Briefly, *E. coli* YG6020 was infected with the phage and spread on M9 salt plates containing Cm and 6-TG, then incubated for 72 hr at 37°C. This enabled selection of colonies harboring a plasmid carrying the gene for chloramphenicol acetyltransferase, as well as a mutated *gpt*. Isolate exhibiting the 6-TG-resistant phenotype was cultured overnight at 37°C in LB broth containing 25 mg/mL Cm, then harvested by centrifugation (7,000 rpm, 10 min), and stored at -80°C.

The mutation spectrum of 6-TG cording sequence were performed by PCR and direct sequencing. Briefly, a 739 bp DNA fragment containing *gpt* was amplified by PCR as described previously [30,53]. Sequencing analysis was done at Takara Bio Inc. (Mie, Japan).

The Spi⁻ assay was performed as described previously [53]. The lysates of Spi⁻ mutants were obtained by infection of *E. coli* LE392 with the recovered Spi⁻ mutants. *gpt* and Spi⁻ MFs were determined in each mouse and the means ± standard deviations were calculated.

Statistical analysis

The data from micronucleus test and *gpt* and Spi⁻ mutation assay are expressed as mean ± standard deviations. The data obtained from comet assay are expressed as mean ± standard errors. The data were statistically compared with the corresponding solvent control using the Student's t-

test for micronucleus and *gpt* and Spi⁻ mutation assay. To test for significant differences of tail moment in the comet assay between a group treated with materials and an untreated group, Dunnett's test after one-way ANOVA was used to evaluate the differences; p values lower than 0.05 were considered to indicate statistical significance.

Abbreviations

CB: carbon black; C_{60}: fullerenes; MN: micronuclei; CNTs: carbon nanotubes; TEM: transmission electron microscope; DLS: dynamic light scattering; MFs: mutant frequencies; 6-TG: 6-thioguanine; 8-oxo-dG: 8-oxo-7,8-dihydro-2'-deoxyguanosin; Iz: imidazolone; Oz: oxazolone; Sp: spiroiminodihydantoin; Gh: guanidinohydantoin; ROS: reactive oxygen species.

Competing interests

The authors declare that they have no competing interests.

Authors' contributions

YT carried out the preparation and performance of *gpt* delta transgenic mouse experiments and drafted the manuscript. SO and MK performed *in vitro* MN tests. TK and SM performed the comet assay. TI, KH and TH performed the animal exposure and *gpt* and Spi⁻ mutation analysis. Pulmonary and renal histopathological evaluations were done by TI and AN. Analysis of size distribution and agglomeration state of particles were done by MW and NF. TN, NK, TY, TS and KW conceived and supervised the study. All authors read and approved the final manuscript.

Acknowledgements

We thank Mr. Naoaki Uchiya, Ms Hiroko Suzuki, Yoko Matsumoto, Naoki Itcho and Mitsuyo Fujii for excellent technical assistance. This study was supported by Grants-in-Aid for Cancer Research and for Research on Risk of Chemical Substances from the Ministry of Health, Labour, and Welfare of Japan. Takashi Higuchi one of authors, is an awardee of a Research Fellowship from the Japan Food Hygiene Association for Promoted Project of Research on Risk of Chemical Substances from the Ministry of Health, Labour, and Welfare of Japan.

References

1. Mazzola L: **Commercializing nanotechnology.** *Nat Biotechnol* 2003, **21**:1137-1143.
2. Paull R, Wolfe J, Hebert P, Sinkula M: **Investing in nanotechnology.** *Nat Biotechnol* 2003, **21**:1144-1147.
3. Elmore AR, Cosmetic Ingredient Review Expert Panel: **Final report on the safety assessment of aluminum silicate, calcium silicate, magnesium aluminum silicate, magnesium silicate, magnesium trisilicate, sodium magnesium silicate, zirconium silicate, attapulgite, bentonite, Fuller's earth, hectorite, kaolin, lithium magnesium silicate, lithium magnesium sodium silicate, montmorillonite, pyrophyllite, and zeolite.** *Int J Toxicol* 2003, **22(Suppl 1)**:37-102.
4. IARC: **Carbon Black and Some Nitro Compounds.** *IARC Monogr Eval Carcinog Risks Hum* 1996, **65**:149-262.
5. Hoet P, Bruske-Hohlfeld I, Salata O: **Possible health impact of nanomaterials.** In *Nanomaterials - Toxicity, health and environmental issues* Edited by: Kumar C. Weinheim: WILEY-VGH Verlag GmbH & Co. KGaA; 2006:53-80.
6. Bosi S, Da Ros T, Spalluto G, Prato M: **Fullerene derivatives: an attractive tool for biological applications.** *Eur J Med Chem* 2003, **38**:913-23.
7. IARC: **Diesel and gasoline engine exhausts and some nitroarenes.** *IARC Monogr Eval Carcinog Risks Hum* 1989, **46**:1-458.
8. Hesterberg TW, Bunn WB 3rd, Chase GR, Valberg PA, Slavin TJ, Lapin CA, Hart GA: **A critical assessment of studies on the carcinogenic potential of diesel exhaust.** *Crit Rev Toxicol* 2006, **36**:727-776.
9. Jacobsen NR, Møller P, Cohn CA, Loft S, Vogel U, Wallin H: **Diesel exhaust particles are mutagenic in FE1-MutaMouse lung epithelial cells.** *Mutat Res* 2008, **641**:54-57.
10. Hashimoto AH, Amanuma K, Hiyoshi K, Sugawara Y, Goto S, Yanagisawa R, Takano H, Masumura K, Nohmi T, Aoki Y: **Mutations in the lungs of gpt delta transgenic mice following inhalation of diesel exhaust.** *Environ Mol Mutagen* 2007, **48**:682-693.
11. Barrett JC, Lamb PW, Wiseman RW: **Multiple mechanisms for the carcinogenic effects of asbestos and other mineral fibers.** *Environ Health Perspect* 1989, **81**:81-89.
12. IARC: **Asbestos.** *IARC Monogr Eval Carcinog Risks Hum* 1997, **14**:11-106.
13. IARC: **Overall Evaluation of Carcinogenicity: An Updating of IARC Monographs.** *IARC Monogr Eval Carcinog Risks Hum* 1987, **1-42(suppl 7)**:106-117.
14. Baan RA: **Carcinogenic hazards from inhaled carbon black, titanium dioxide, and talc not containing asbestos or asbestiform fibers: recent evaluations by an IARC Monographs Working Group.** *Inhal Toxicol* 2007, **19(Suppl 1)**:213-228.
15. IARC: **Man-made Vitreouis Fibres.** *IARC Monogr Eval Carcinog Risks Hum* 2002, **81**:33-374.
16. Bunn WB 3rd, Bender JR, Hesterberg TW, Chase GR, Konzen JL: **Recent studies of man-made vitreous fibers. Chronic animal inhalation studies.** *J Occup Med* 1993, **35**:101-113.
17. Lam C-W, James JT, McCluskey R, Holian A, Hunter RL: **Toxicity of carbon nanotubes and its implications for occupational and environmental health.** In *Nanomaterials - Toxicity, health and environmental issues* Edited by: Kumar C. Weinheim: WILEY-VGH Verlag GmbH & Co. KGaA; 2006:130-152.
18. Donaldson K, Aitken R, Tran L, Stone V, Duffin R, Forrest G, Alexander A: **Carbon nanotubes: a review of their properties in relation to pulmonary toxicology and workplace safety.** *Toxicol Sci* 2006, **92**:5-22.
19. Poland CA, Duffin R, Kinloch I, Maynard A, Wallace WA, Seaton A, Stone V, Brown S, Macnee W, Donaldson K: **Carbon nanotubes introduced into the abdominal cavity of mice show asbestos-like pathogenicity in a pilot study.** *Nat Nanotechnol* 2008, **3**:423-428.
20. Takagi A, Hirose A, Nishimura T, Fukumori N, Ogata A, Ohashi N, Kitajima S, Kanno J: **Induction of mesothelioma in p53+/- mouse by intraperitoneal application of multi-wall carbon nanotube.** *J Toxicol Sci* 2008, **33**:105-116.
21. Nielsen GD, Roursgaard M, Jensen KA, Poulsen SS, Larsen ST: **In vivo biology and toxicology of fullerenes and their derivatives.** *Basic Clin Pharmacol Toxicol* 2008, **103**:197-208.
22. Jensen AW, Wilson SR, Schuster DI: **Biological applications of fullerenes.** *Bioorg Med Chem* 1996, **4**:767-779.
23. Nohmi T, Masumura K: **Molecular nature of intrachromosomal deletions and base substitutions induced by environmental mutagens.** *Environ Mol Mutagen* 2005, **45**:150-161.
24. Nohmi T, Suzuki M, Masumura K, Yamada M, Matsui K, Ueda O, Suzuki H, Katoh M, Ikeda H, Sofuni T: **Spi(-) selection: An efficient method to detect gamma-ray-induced deletions in transgenic mice.** *Environ Mol Mutagen* 1999, **34**:9-15.
25. Xu A, Chai Y, Hei T: **Genotoxic responses to titanium dioxide nanoparticles and fullerene in gpt delta transgenic MEFcells.** *Particle Fibre Toxicol* 2009, **6**:3.
26. Negishi K, Hao W: **Spectrum of mutations in single-stranded DNA phage M13mp2 exposed to sunlight: predominance of G-to-C transversion.** *Carcinogenesis* 1992, **9**:1615-1618.
27. Akasaka S, Yamamoto K: **Hydrogen peroxide induces G:C to T:A and G:C to C:G transversions in the supF gene of Escherichia coli.** *Mol Gen Genet* 1994, **243**:500-505.
28. Valentine MR, Rodriguez H, Termini J: **Mutagenesis by peroxy radical is dominated by transversions at deoxyguanosine: evidence for the lack of involvement of 8-oxo-dGI and/or abasic site formation.** *Biochemistry* 1998, **37**:7030-7038.

29. Shin CY, Ponomareva ON, Connolly L, Turker MS: **A mouse kidney cell line with a G:C --> C:G transversion mutator phenotype.** *Mutat Res* 2002, **503:**69-76.
30. Jacobsen NR, Pojana G, White P, Møller P, Cohn CA, Korsholm KS, Vogel U, Marcomini A, Loft S, Wallin H: **Genotoxicity, cytotoxicity, and reactive oxygen species induced by single-walled carbon nanotubes andC(60) fullerenes in the FE1-Muta™ Mouse lung epithelial cells.** *Environ Mol Mutagen* 2008, **49:**476-487.
31. Valberg PA, Long CM, Sax SN: **Integrating studies on carcinogenic risk of carbon black: epidemiology, animal exposures, and mechanism of action.** *J Occup Environ Med* 2006, **48:**1291-1307.
32. Sayes CM, Marchione AA, Reed KL, Warheit DB: **Comparative pulmonary toxicity assessments of C60 water suspensions in rats: few differences in fullerene toxicity in vivo in contrast to in vitro profiles.** *Nano Lett* 2007, **7:**2399-2406.
33. Gao N, Keane MJ, Ong T, Wallace WE: **Effects of simulated pulmonary surfactant on the cytotoxicity and DNA-damaging activity of respirable quartz and kaolin.** *J Toxicol Environ Health A* 2000, **60:**153-167.
34. Kasai H, Nishimura S: **DNA damage induced by asbestos in the presence of hydrogen peroxide.** *Gann* 1984, **75:**841-844.
35. Aust A: **The role of iron in asbestos induced cancer.** In *Cellular and Molecular Effects of Mineral and Syntheticn Dusts and Fibers, NATO ASI Series Volume H85.* Edited by: Davis JMG, Jaurand M-C. Berlin: Springer-Verlag; 1994:53-61.
36. Mossman BT, Gee BL: **Pulmonary reactions and mechanisms of toxicity of inhaled fibers.** In *Toxicology of the Lung* 2nd edition. Edited by: Gardner, et al. New York: Raven Press; 1993:371-387.
37. Shibutani S, Takeshita M, Grollman AP: **Insertion of specific bases during DNA synthesis past the oxidation-damaged base 8-oxodG.** *Nature* 1991, **349:**431-434.
38. Moriya M: **Single-stranded shuttle phagemid for mutagenesis studies in mammalian cells: 8-oxoguanine in DNA induces targeted G.C-->T.A transversions in simian kidney cells.** *Proc Natl Acad Sci USA* 1993, **90:**1122-1126.
39. Kornyushyna O, Berges AM, Muller JG, Burrows CJ: **In vitro nucleotide misinsertion opposite the oxidized guanosine lesions spiroiminodihydantoin and guanidinohydantoin and DNA synthesis past the lesions using Escherichia coli DNA polymerase I (Klenow fragment).** *Biochemistry* 2002, **41:**15304-15314.
40. Cadet J, Berger M, Buchko GW, Joshi PC, Raoul S, Ravanat JL: **2,2-Diamino-4-[(3,5-di-O-acetyl-2-deoxy-.beta.-D-erythro- pentofuranosyl)amino]-5-(2H)-oxazolone: a Novel and Predominant Radical Oxidation Product of 3',5'-Di-O-acetyl-2'-deoxyguanosine.** *J Am Chem Soc* 1994, **116:**7403-7404.
41. Goyal RN, Jain N, Garg DK: **Electrochemical and enzymic oxidation of guanosine and 8-hydroxyguanosine and the effects of oxidation products in mice.** *Bioelectrochemistry and Bioenergetics* 1997, **43:**105-114.
42. Ye Y, Muller JG, Luo W, Mayne CL, Shallop AJ, Jones RA, Burrows CJ: **Formation of 13C-, 15N-, and 18O-labeled guanidinohydantoin from guanosine oxidation with singlet oxygen. Implications for structure and mechanism.** *J Am Chem Soc* 2003, **125:**13926-13927.
43. Burrows CJ, Muller JG, Kornyushyna O, Luo W, Duarte V, Leipold MD, David SS: **Structure and potential mutagenicity of new hydantoin products from guanosine and 8-oxo-7,8-dihydroguanine oxidation by transition metals.** *Environ Health Perspect* 2002, **110(Suppl 5):**713-717.
44. Kino K, Sugiyama H: **UVR-induced G-C to C-G transversions from oxidative DNA damage.** *Mutat Res* 2005, **571:**33-42.
45. Kino K, Sugiyama H: **Possible cause of G-C-->C-G transversion mutation by guanine oxidation product, imidazolone.** *Chem Biol* 2001, **8:**369-378.
46. Kino K, Ito N, Sugasawa K, Sugiyama H, Hanaoka F: **Translesion synthesis by human DNA polymerase eta across oxidative products of guanine.** *Nucleic Acids Symp Ser* 2004, **48:**171-172.
47. Hailer MK, Slade PG, Martin BD, Sugden KD: **Nei deficient Escherichia coli are sensitive to chromate and accumulate the oxidized guanine lesion spiroiminodihydantoin.** *Chem Res Toxicol* 2005, **18:**1378-1383.
48. Matter B, Malejka-Giganti D, Csallany AS, Tretyakova N: **Quantitative analysis of the oxidative DNA lesion, 2,2-diamino-4-(2-deoxy-beta-D-erythro-pentofuranosyl)amino]-5(2H)-oxazolone (oxazolone), in vitro and in vivo by isotope dilution-capillary HPLC-ESI-MS/MS.** *Nucleic Acids Res* 2006, **34:**5449-5460.
49. Justice MJ, Noveroske JK, Weber JS, Zheng B, Bradley A: **Mouse ENU mutagenesis.** *Hum Mol Genet* 1999, **8:**1955-1963.
50. Rojas E, Lopez MC, Valverde M: **Single cell gel electrophoresis: methodology and applications.** *Journal of Chromatography B* 1999, **722:**225-254.
51. Park EJ, Yoon J, Choi K, Yi J, Park K: **Induction of chronic inflammation in mice treated with titanium dioxide nanoparticles by intratracheal instillation.** *Toxicology* 2009, **260:**37-46.
52. Kaewamatawong T, Shimada A, Okajima M, Inoue H, Morita T, Inoue K, Takano H: **Acute and subacute pulmonary toxicity of low dose of ultrafine colloidal silica particles in mice after intratracheal instillation.** *Toxicol Pathol* 2006, **34:**958-65.
53. Sasaki YF, Tsuda S, Izumiyama F, Nishidate E: **Detection of chemically induced DNA lesions in multiple mouse organs (liver, lung, spleen, kidney, and bone marrow) using the alkaline single cell gel electrophoresis (Comet) assay.** *Mutat Res* 1997, **388:**33-44.
54. Toyoizumi T, Deguchi Y, Masuda S, Kinae N: **Genotoxicity and estrogenic activity of 3,3'-dinitrobisphenol A in goldfish.** *Biosci Biotechnol Biochem* 2008, **72:**2118-2123.
55. Nohmi T, Suzuki T, Masumura K: **Recent advances in the protocols of transgenic mouse mutation assays.** *Mutat Res* 2000, **455:**191-215.

Original Article

Cytogenetic and Genome Research

Cytogenet Genome Res 2009;125:201–212
DOI: 10.1159/000230004

Accepted after revision: March 13, 2009
by M. Schmid

The Chromosomal Constitution of Postmitotic Neurons, Assessed by Neuronal Nuclear Transfer into Oocytes and in ES Cell Lines Derived from Them

T. Osada[a–c] N. Kakazu[d] M. Watanabe[e] H. Yamane[d] T. Yagi[b, c]

[a]Department of Regenerative and Developmental Biology, Mitsubishi Kagaku Institute for Life Sciences (MITILS), Tokyo; [b]CREST Research Agency, JST, [c]KOKORO Biology Group, Department of Integrated Biology, Graduate School of Frontier Biosciences, Osaka University, Osaka; [d]Department of Environmental and Preventive Medicine, Shimane University School of Medicine, Izumo City; [e]Laboratory for Medical Engineering, Division of Materials Science and Chemical Engineering, Graduate School of Engineering, Yokohama National University, Yokohama, Japan

Key Words
Chromatin condensation · Chromosomes · Embryonic stem cells · Nuclear transfer · SKY

Abstract
Spectral karyotyping (SKY) was used to assess the chromosomal constitution of embryos generated by nuclear transfer (NT) of neuronal nuclei (N-NT) or cumulus cell nuclei (C-NT) into oocytes and of their embryonic stem cell derivatives (ntES cells). We detected chromosomal changes during the first mitotic cleavage and in the condensed chromatids of NT embryos. We also found clonal translocations in the ntES cells that were derived from NT embryos cloned from neuronal nuclei. The differentiation potentials of the ntES cells showing chromosomal rearrangements were partly restricted. Our findings indicate that balanced or unbalanced chromosomal translocations can occur in early NT embryogenesis, suggesting that a DNA repair system is activated during both NT embryogenesis and ntES cell establishment. We observed a higher incidence of chromosomal changes in N-NT than in C-NT embryos, which may reflect a higher frequency of double-stranded (ds) DNA breaks in the neuronal genome.

Although condensed chromosomes are not visible in postmitotic cells, technology allowing the visualization of whole chromosome sets provides important genetic information about DNA mutations associated with physiology and disease. A wealth of studies has indicated that chromosomes are susceptible to age-related DNA damage [Johnson et al., 1999; Albert et al., 2002] and cell death [Gossen et al., 1989]. DNA variation among individuals was recently discovered and put forward as a mechanism for genetic diversity [Redon et al., 2006]. Although DNA recombination in the neuronal genome, analogous to that occurring in the immune system, has been postulated to contribute to neuronal identity [Chun et al., 1991], no definitive evidence for this activity has been reported. Instead, recent analyses have reported chromosomal aneuploidy in neural subpopulations [Rehen et al., 2001] and the integration of retrotransposable elements in CNS cells [Muotri et al., 2005]. Although the biological significance of these discoveries remains unclear, they are fascinating phenomena with potentially significant implications for neuronal complexity [Mattick and Mehler, 2008]. To analyze the genetic codes of individual neurons, however, a genetic source, i.e. a large collection of cell lines cloned from the DNA of single neurons, is needed.

KARGER

Fax +41 61 306 12 34
E-Mail karger@karger.ch
www.karger.com

1424–8581/09/1253–0201$26.00/0

Accessible online at:
www.karger.com/cgr

Tomoharu Osada, DVM, PhD
Department of Regenerative and Developmental Biology
Mitsubishi Kagaku Institute of Life Sciences
11 Minamiooya, Machida-shi, Tokyo 194-8511 (Japan)
Tel. +81 42 724 6250, Fax +81 42 724 6314, E-Mail tomoosada@gmail.com

Table 1. SKY analysis of nuclear transferred ES cell lines

ES cell line	Donor nuclei	Strain	Sex	Karyotypes		
				analyzed	normal (%)	clonal translocation [n, %]
Cam-1	pyramidal neurons	C57Bl/6 × [(C57Bl/6 × DBA/2) × DBA/2]N2	XY	4	2 (50)	
Cam-2	pyramidal neurons	C57Bl/6 × [(C57Bl/6 × DBA/2) × DBA/2]N2	XY	17	10 (59)	T(11;13) [4, 23]
Nex-1	pyramidal neurons	C57Bl/6 × [(C57Bl/6 × DBA/2) × DBA/2]N3	XY	18	12 (67)	
Nex-2	pyramidal neurons	C57Bl/6 × [(C57Bl/6 × DBA/2) × DBA/2]N3	XY	12	0 (0)	T(1;6); der(4)T(4;6) [12, 100]
Gad67-1	GABAnergic neurons	DBA/2 × C57Bl/6	XY	19	12 (63)	
Gad67-2	GABAnergic neurons	DBA/2 × C57Bl/6	XX	5	1 (20)	
Cum-1	cumulus cells	DBA/2 × C57Bl/6	XX	10	2 (20)	
TT2		CBA × C57Bl/6	XY	10	6 (60)	

Several methodologies have been developed to analyze single cell-derived DNA. First, a transgenic mouse mutation detection system was developed to assess directly mutations in the genome of postmitotic cells in vivo [Gossen et al., 1989]. This approach enables the detection of radiation-induced DNA damage in somatic cells, but it may not be able to disclose site-specific mutations in the genome. An alternative approach was developed to visualize the entire chromosomal constitution of a single postmitotic cell by means of nuclear transfer (NT) [Osada et al., 2002]. In the original experiment, mammalian oocytes were used as a biological container in which to examine the chromosome constitution of sperm [Rudak et al., 1978; Lee et al., 1996]. We previously applied NT to the analysis of neuronal genomes [Osada et al., 2002], and our findings suggested that chromosomal changes could occur in embryos generated by NT of neuronal nuclei (N-NT embryos) during the first mitotic cleavage. In the present study, we used spectral karyotyping (SKY) [Liyanage et al., 1996] to examine the karyotypes of N-NT embryos during condensed chromatid formation and the first mitotic cleavage, and of those cell lines derived from N-NT embryos.

Materials and Methods

Mice and ES Cells

Recipient oocytes were collected from B6D2F1 hybrid mice. Donor neurons were collected from B6 transgenic mice that expressed green fluorescence protein (GFP) specifically in pyramidal neurons resulting from the use of a genetic marking system [Osada et al., 2005]. Six ntES cell lines derived from the nuclei of neurons (Cam-1, -2, Nex-1, -2, and Gad67-1, -2) and 1 ntES cell line from cumulus cells (Cum-1) were examined in this study (table 1). These cells were cultivated with feeder cells and TT2 ES cells were used as control. The TT2 ES cells were derived from blastocysts of an F1 hybrid mouse strain (CBA × C57BL/6) and showed pluripotency in chimeras, including the ability to form germ lines [Yagi et al., 1993].

Nuclear Transfer and Mitotic Spread Preparation

Nuclear transfer experiments were carried out as described previously [Osada et al., 2005]. To obtain the condensed chromatids, cells were collected and fixed 2–3 h after injection of the donor nuclei into enucleated oocytes. To obtain metaphase chromosomes, NT embryos during the first mitotic cleavage, and ES cells derived from NT embryos were collected (fig. 1). Metaphase spreads from the N-NT embryos were prepared with a standard method [Mikamo et al., 1983]. The zona pellucida of the N-NT oocytes was digested with actinase (Kaken Pharmaceutical Co., Ltd., Tokyo, Japan). After washing with PBS, the cells were transferred to a hypotonic solution (0.075 mM citric acid:10% FBS, 1:1). The expanded cells were fixed with modified Carnoy's fixative and promptly spread on glass slides. To obtain mitotic spreads from the first cleavage, the N-NT embryos were incubated for 6–7 h after activation in CZB medium containing 6 nM vinblastine sulfate.

ES Cell Culture

ES cells were cultured and maintained under standard conditions [Hogan et al., 1994]. The culture medium for cloned ES cells was composed of 17.5% KnockOut Serum Supplement (KSR), 100 μM non-essential amino acids, 1 mM pyruvate (all from Invitrogen, Carlsbad, CA), 0.1 mM β-mercaptoethanol (Wako, Osaka, Japan), and 1,000 IU/ml leukemia inhibitory factor (LIF) in KnockOut D-MEM (Invitrogen). The TT2 ES cells were cultured in the same medium with the same components, except that 20% fetal bovine serum (Invitrogen) was used instead of KSR. The feeder cells were prepared from embryonic fibroblasts obtained from a BALB/c inbred mouse strain on embryonic day (E) 13.5 and treated with 10 μg/ml mitomycin C (Sigma, St. Louis, MO) for at least 2 h. The cells were passaged approximately every 4 days.

Metaphase Spread Preparation

After 6–9 passages ES cells at metaphase were used for the preparation of metaphase spreads with a standard method [Kakazu et al., 1999]. The ES cells were treated with colcemid (Invitrogen) at 0.1 μg/ml final concentration for 1 h. Mitotically arrested cells were subjected to hypotonic treatment (0.075 M KCl)

for 30 min, fixed by changing the solution with Carnoy's fixative (methanol:acetic acid = 3:1, v/v) 3 times, after which the solution containing the cells was spread on a glass slide.

Spectral Karyotyping (SKY)

The metaphase cells were subjected to SKY analysis. The mouse SKY paint probe mixture (Applied Spectral Imaging, Migdal Ha'Emek, Israel), which contains combinatorially labeled painting probes specific for each of the 21 mouse chromosomes, was used for hybridization. Hybridization and detection were carried out as described elsewhere [Kakazu et al., 1999]. The chromosomes were counterstained with 4′,6-diamidino-2-phenylindole dihydrochloride (DAPI).

Fluorescence in situ Hybridization (FISH) Analyses

To narrow down the 6q breakpoint region of T(1;6) in the Nex-2 NT-ES cells, we performed sequential FISH analyses using 11 bacterial artificial chromosome (BAC) probes located on chromosome 6q. The BAC clones (RP23 series) on chromosome 6q were selected according to the University of California Santa Cruz (UCSC) Genome Browser (http://genome.ucsc.edu), and were directly labeled with SpectrumOrange-dUTP (Abbott Molecular/Vysis, Des Plaines, IL). To identify normal and translocated chromosomes 1, RP23-374B10 (located at chromosome 1qA1) labeled with SpectrumOrange-dUTP (Abbott Molecular/Vysis) was used together with the chromosome 6q probes. Hybridization, washing, and detection were performed as described previously [Kakazu et al., 1999]. Chromosomes were counterstained with DAPI. FISH images were captured and analyzed with the PowerGene system (Applied Imaging).

Differentiation of ES Cells in vitro and in vivo

The differentiation of ES cells in vitro was induced by retinoic acid, as described previously [Bain et al., 1995]. Briefly, after 2 days in vitro, the ES cells were trypsinized and dispersed into the culture medium without LIF or β-mercaptoethanol and with trans-retinoic acid (1 μM, Sigma). On the 4th day after addition of the retinoic acid, the embryoid bodies (EBs) that had developed were transferred onto a laminin/poly-L-lysine (1:1)-coated Petri dish containing the same medium, but without retinoic acid. The cells were collected and analyzed after 7 days of culture.

For the subcutaneous injection of ES cells into nude mice, ES cells were grown under normal conditions for 3 days. The cells were then gently trypsinized, and 1–2 × 10^6 cells were injected subcutaneously into each flank of 6–8-week-old female BALB/c *nu/nu* mice (Oriental Yeast, Tokyo, Japan). 3–5 weeks after injection, the mice were euthanized, decapitated and the tumors collected. The obtained tumors were weighed and fixed with either 10% neutralized formalin solution or Bouin's solution.

Immunofluorescence

Indirect immunofluorescence analyses of the differentiated cells were performed on the 8th day of culture on a laminin/lysine-coated Petri dish, and of undifferentiated cells on the 4th day of culture with feeder cells. The cells were fixed with 4% paraformaldehyde for 30 min at room temperature (RT) and then permeabilized with PBS containing 0.05% Tween-20 and 0.5% Triton X-100 for 20 min at RT. After blocking with PBS containing 0.05% Tween-20 and 10% normal goat serum for 1 h, the cells were incubated with antibodies to NeuN (1:100, Chemicon International, Temecula, CA), GAD67 (1:400, Chemicon), or Desmin (1:50, Sigma) overnight. After incubation with the secondary antibodies, which were conjugated with Alexafluor 594 (Molecular Probes, Eugene, OR), the cells were stained with DAPI and observed under a fluorescence microscope (IX51; Olympus, Tokyo, Japan).

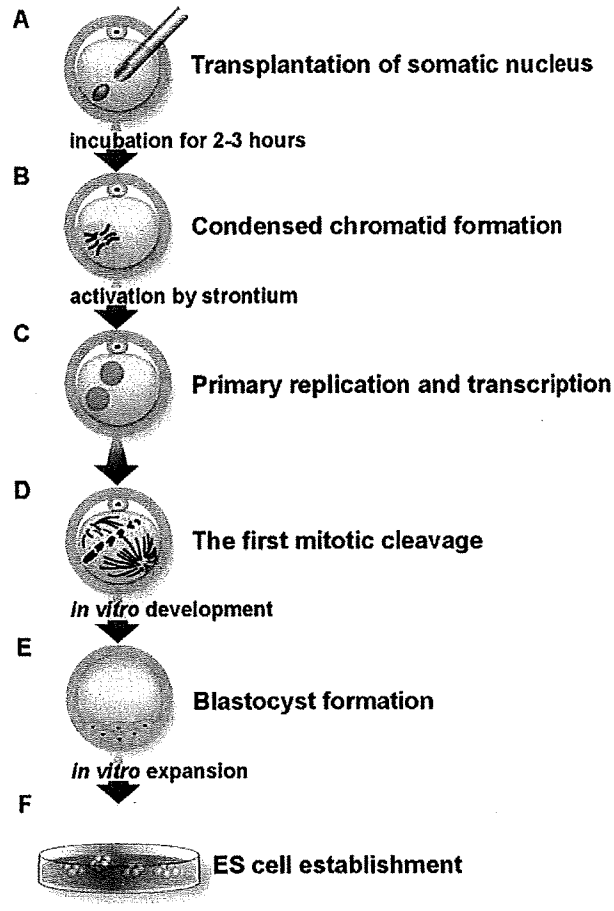

Fig. 1. Diagram of the developmental stages at which condensed chromatids/chromosomes were examined. After its injection into the ooplasm (**A**), donor nuclear DNA condenses within 2–3 h (**B**). Because the injected DNA is not replicated during this period, the DNA forms condensed chromatids. After activation stimulation by strontium, the reconstructed NT embryos form pseudo-pronuclei where the primary replication and transcription progress (**C**). Mitotic spreads are prepared during the first embryonic cleavage (**D**). Some of the N-NT embryos develop into blastocysts (**E**). The inner cell mass is expanded in vitro, and the N-ntES cells are established after sequential passages (**F**). Mitotic spreads are prepared from the N-ntES cells after 6–9 passages.

Table 2. SKY analysis of chromosomes from the N-NT and C-NT embryos during the first cleavage

Donor cells	No. of karyotypes analyzed	No. of informative karyotypes	No. (%) of normal karyotypes	Abnormal karyotypes	
				aneuploidy (indicated by number of chromosomes)	translocation (indicated by karyotypes)
Cortical neurons (N-NT)	87	25	20 (80)	36, 38, 39	T(1;12); T(6;13)
Cumulus cells (C-NT)	35	10	9 (90)	39	

Table 3. G-banding analysis of enucleated oocytes 3 h after injection of cumulus cell nuclei and adult cortical neuronal nuclei

Donor cells	No. of PCC analyzed	No. (%) of normal PCC	No. (%) of abnormal PCCs							
			with chromosome fragment			without chromosome fragment		with undercondensed chromatids		
			40 chr. (SA)	<40 chr.	>40 chr. (SA + NA)	<40 chr. (NA)	>40 chr. (NA)	<40 chr.	40 chr.	>40 chr.
Cortical neurons	92	47 (51)[a]	9 (10)	14 (15)[b]	1 (1)	17 (18)	2 (2)	1 (1)	1 (1)	0 (0)
Cumulus cells	48	39 (81)[a]	6 (13)	0 (0)[b]	0 (0)	3 (6)	0 (0)	0 (0)	0 (0)	0 (0)

Abbreviations: PCC, premature chromosome condensation; SA, structural chromosome aberrations; NA, numerical chromosome aberrations (aneuploidy).
[a] $p < 0.005$; [b] $p < 0.01$.

Reverse Transcription Polymerase Chain Reaction (RT-PCR)

Total RNA was isolated from each ES cell line (4-day cultures) and their derivatives (8-day culture on a laminin/lysine-coated Petri dish) by Trizol Reagent (Invitrogen). The cDNA was synthesized with the aid of Superscript III (Invitrogen) using oligo(dT)$_n$ primers, according to the manufacturer's instructions. The synthesized DNA was amplified as follows: 1 min at 94°C, then 30 cycles of 30 s at 94°C, 30 s at 55°C, and 1 min at 72°C, followed by a 10-min extension at 72°C. Hypoxanthine guanine phosphoribosyl transferase 1 *(Hprt1)* was used as a positive control. The primer sequences used for this assay and the length of the amplified DNA fragments were as follows:

POU domain, class 5, transcription factor 1 *(Pou5f1*, synonym *Oct-3/4)*: F 5′-CTTCTGCAGGGCTTTCATGT-3′, R 5′-TGTGGACCTCAGGTTGGACT-3′, 72 bp. Alpha-fetoprotein *(Afp)*: F 5′-ACCAGACCTTAGGAGACTAC-3′, R 5′-CACTCTTCCTTCTGGAGATG-3′, 596 bp. Transthyretin *(Ttr)*: F 5′-AAATCGTACTGGAAGACACT-3′, R 5′-ACTCTGCTTTCTGACCTATC-3′, 510 bp. Myosin heavy chain cardiac muscle 6 *(Myh6)*: F 5′AGATGCACTGGAGAAGTCTG-3′, R 5′-CAGCCATCTCCTCTGTTAGG-3′, 371 bp. Glial fibrillary acid protein *(Gfap)*: F 5′-CAAACACGAAGCTAACGACT-3′, R 5′-CCACAGTCTTTACCACGATG-3′, 407 bp. Glutamate receptor; ionotropic, AMPA1 (alpha1) *(Gria1)*: F 5′-CCAATTTGAAGGCAATGACC-3′, R 5′-TCTTCTCAAACACAGCGATT-3′, 770 bp. Gamma-aminobutyric acid (GABA) A receptor, subunit beta 1 *(Gabrb1)*: F 5′-GGGGCTTCTCTCTTTTCCCGTGA-3′, R 5′-GGTGTCTGGTACCCAGAGTTGGT-3′, 334 bp. *Hprt1*: F 5′-TTGTTGGATATGCCCTTGAC-3′, R 5′-GGAAATCGAGAGCTTCAGAC-3′, 506 bp.

Aliquots (5 μl) of the PCR mixture were analyzed by electrophoresis on 1–1.5% agarose gels stained with 0.5 μg/ml ethidium bromide.

Results

SKY Analyses during the First Mitotic Cleavage of N-NT Embryos

We first wanted to examine if the chromosomal changes in the N-ntES cells were detectable in early development. To this end, metaphase spreads prepared during the first mitotic cleavage of the N-NT and C-NT embryos were subjected to SKY analysis. Aneuploidy was detected in both the N-NT and C-NT embryos. In contrast to our previous findings [Osada et al., 2002] the frequency of aneuploidy in the N-NT and C-NT embryos was similar (table 2). On the other hand, a balanced translocation between chromosomes 6 and 13, T(6;13) (data not shown), and a balanced translocation between chromosomes 1 and 12, T(1;12) (fig. 2), were observed in the N-NT embryos

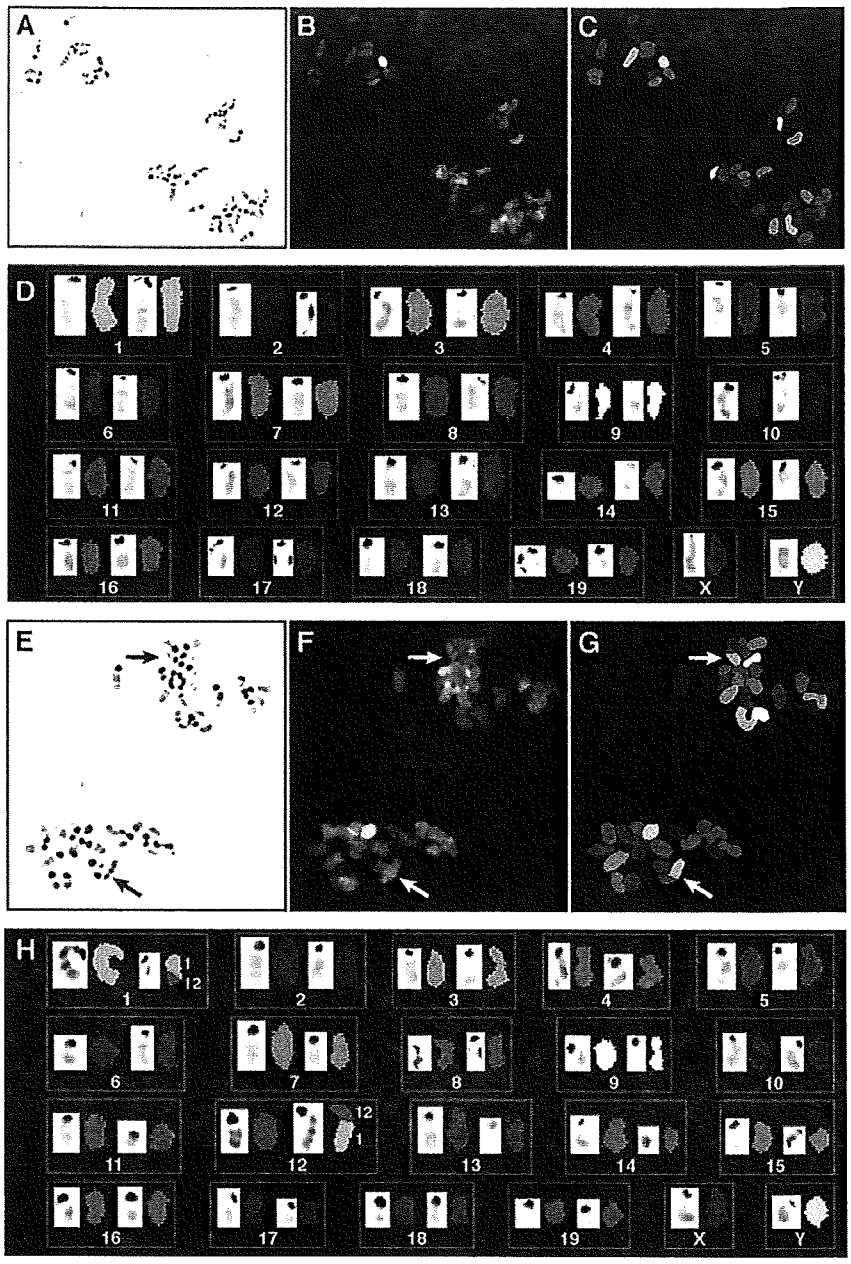

Fig. 2. SKY analysis of eggs at the first mitosis after injection of nuclei from adult cerebral neurons. **A–D** Metaphase spread with a normal chromosome set. **E–H** Metaphase spread with a balanced translocation between chromosomes 1 and 12, T(1;12). Images from left to right show inverted DAPI (**A**, **E**), spectral color (**B**, **F**), and classification color images (**C**, **G**). **D**, **H** Karyotype tables produced by combining SKY and DAPI banding. For each chromosome in the tables, G-band-like images are shown on the left and classified color images on the right. The numbers next to the classification color images in **H** indicate the origin of the chromosomal material. **E–G** Arrows indicate chromosomes with T(1;12).

(table 2), whereas no chromosomal changes were detected in the mitotic spreads prepared from the C-NT embryos.

SKY Analyses of the Condensed Chromatids after Injection of a Neuronal or Cumulus Cell Nucleus

Chromosomes from somatic cell nuclei form chromatid-like structures in the ooplasm upon their transfer into enucleated oocytes via M-phase promoting factor (MPF) [Ziegler and Masui, 1973]. Since this appears to be a biological window for assessment, prior to SKY analysis of the karyotype of donor nuclei by NT with a minimal influence from oocyte factors, aneuploidy of the chromatids was assessed by means of Giemsa staining (table 3). Fragmentation was observed in the chro-

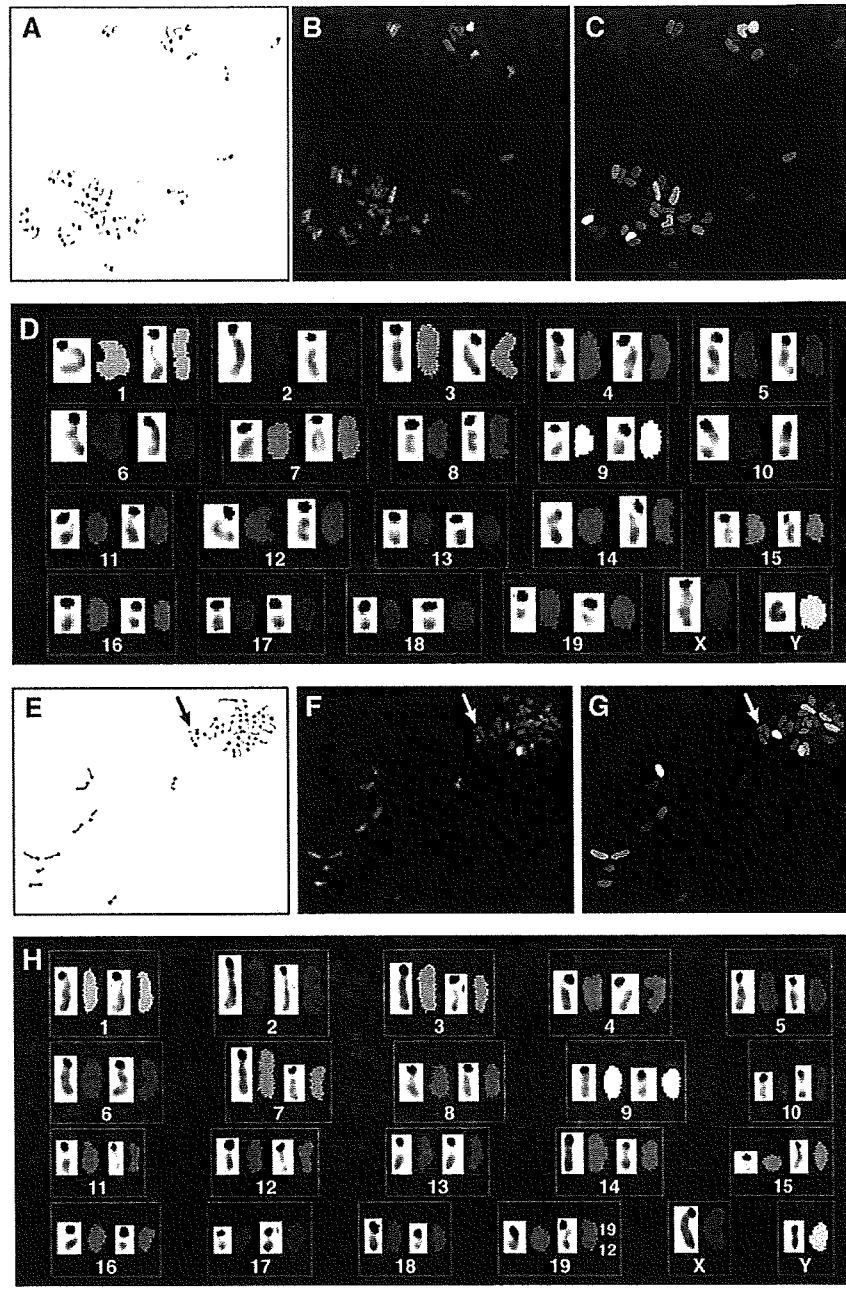

Fig. 3. SKY analysis of the condensed chromatids of oocytes injected with the nuclei of adult cerebral neurons. **A–D** Metaphase spread of a nucleus-injected oocyte without chromosomal aberrations. **E–H** Metaphase spread with an abnormal set of condensed chromatids of an oocyte injected with a neuronal nucleus. Note the presence of an unbalanced translocation, der(19)T(12;19) (**H**), indicated by arrows in **E–G**. For arrangement of images see legend of figure 2.

matid preparations from oocytes bearing neuronal or cumulus cell nuclei. A loss of chromosomes was observed in the neuron-derived condensed chromatids as reported previously [Osada et al., 2002]. Undercondensed chromatin was also detected, but with a lower frequency than in our previous study [Osada et al., 2002]. SKY painting of the chromatid preparations (fig. 3) showed the presence of unbalanced chromosomal changes in 3 of the 23 metaphase cells analyzed among the oocytes bearing a neuronal nucleus, including 2 showing an unbalanced translocation between chromosomes 12 and 19 (table 4, fig. 3E–H). This translocation

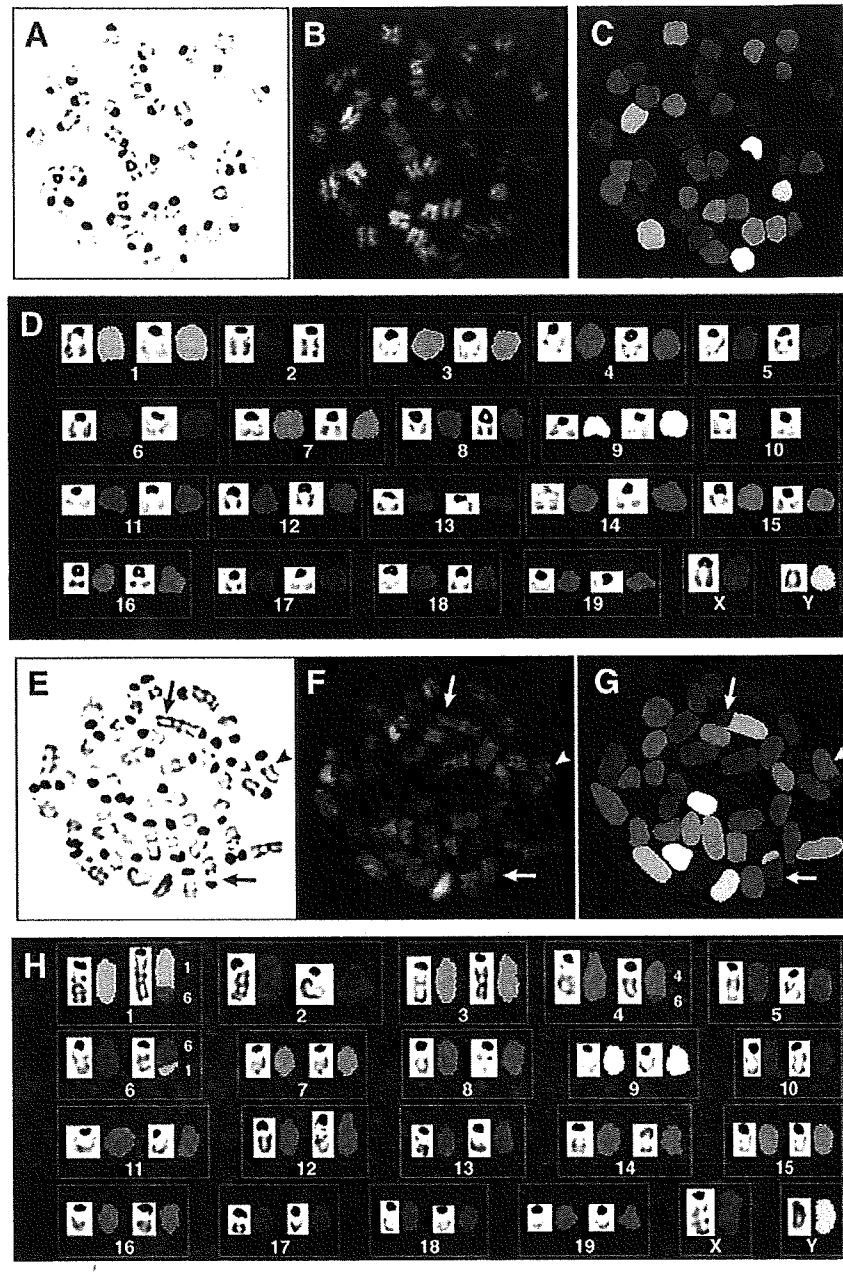

Fig. 4. SKY analysis of N-ntES cell lines Cam-2 (**A–D**) and Nex-2 (**E–H**). Arrows indicate chromosomes with a balanced translocation between chromosomes 1 and 6, T(1;6), arrowheads indicate the derivative chromosome 4 with an unbalanced translocation between chromosomes 4 and 6, der(4)T(4;6) (**E–G**). For arrangement of images see legend of figure 2.

Table 4. SKY analysis of premature chromatin condensations in the enucleate oocytes 3 h after injection

Donor cells	No. of PCC analyzed	No. of informative PCC	No. (%) of normal PCC	Abnormal PCC		
				fragments (indicated by number of karyotypes)	aneuploidy [n] (indicated by number of chromosomes)	translocation [n] (indicated by karyotypes)
Cortical neurons	93	23	17 (74)	2	36 [2]	der(19)T(12;19) [2]
Cumulus cells	47	15	13 (87)	0	39, 36	

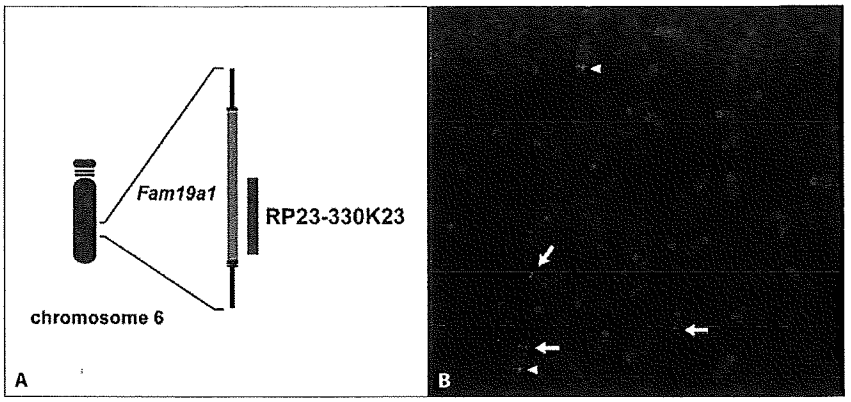

Fig. 5. A Schematic representation of the *Fam19a1* genomic region on mouse chromosome 6 and the position of the BAC probe RP23-330K23 used in this FISH analysis. **B** FISH analysis using the green-labeled RP23-330K23 probe (6qD3; arrows) together with the red-labeled RP23-374B10 probe (1qA1; arrowheads). Split green signals are detected on both the derivative chromosomes 1 and 6 in addition to the green signal on normal chromosome 6 in metaphases from Nex-2 NT-ES cells, indicating that RP23-330K23 spans the 6q breakpoint of T(1;6). The RP23-374B10 probe (red signal) was used for identification of normal and translocated chromosomes 1.

resulted in partial trisomy of the distal end of chromosome 12.

SKY Karyotyping of the ntES Cells Derived from N-NT Embryo (N-ntES) cells

We also used ntES cells derived from N-NT embryos at metaphase for SKY karyotyping [Osada et al., 2005]. SKY analysis of 8 ntES cell lines detected 2 clonal chromosomal abnormalities in Cam-2 and Nex-2 ntES cell lines (table 1). SKY analysis of the Cam-2 ES cells identified a normal karyotype in the majority of metaphases (59%) (fig. 4A–D) and 1 clonal balanced translocation, T(11;13) (data not shown), in another population of metaphase cells. SKY analysis of Nex-2 cells revealed a balanced translocation, T(1;6), and a derivative chromosome 4, der(4)T(4;6), from an unbalanced translocation between chromosomes 4 and 6 in all metaphase cells analyzed (fig. 4E–H). In contrast, no obvious clonal chromosomal abnormalities were detected in the control TT2 ES cells. The karyotypes of the Nex-1 line were normal in the major metaphase population (67%). Another population showed aneuploidy, with chromosomal numbers ranging from 46 to 76. Besides the structural and numerical chromosomal changes, the SKY analyses also detected metaphases with separated sister chromatids, also known as premature chromatid separation (PCS) [Hogan et al., 1994] in 5 ES cell lines (online supplementary fig. S1; for online supplementary material, see www.karger.com/doi/000230004).

FISH Analyses

The 6q breakpoint region of T(1;6) in the Nex-2 NT-ES cells was narrowed down by FISH analyses with 11 BAC probes located at chromosome 6q. The results demonstrated that the BAC clone RP23-330K23 (located at 6qD3) spanned the 6q breakpoint of T(1;6) (fig. 5).

Normal Differentiation Potentials of N-ntES Cells with Karyotypic Changes

All ES cells examined were positive for alkaline phosphatase activity (fig. 6A) and Oct-3/4 immunoreactivity (data not shown), indicating that the ntES cells were in an undifferentiated state. ES cells treated with retinoic acid and cultured without LIF or feeder cells differentiated into ectoderm, neurons, mesodermal fibroblast-like cells, and parietal endoderm-like cells (fig. 6B). The morphological observations were verified by indirect immunofluorescence using the ectodermal neuronal markers NeuN and GAD67 (fig. 6C, D) and the mesodermal marker desmin (fig. 6E).

The differentiation potentials of the ntES cells were characterized by means of RT-PCR analyses. The *Pou5f1* gene was expressed in all undifferentiated ES cells. Differentiated EB cells, induced by retinoic acid, expressed several somatic cell-lineage marker genes: *Afp* and *Ttr* genes as endoderm markers; *Myh6* as a mesoderm marker; and *Gfap, Gria1*, and *Gabrb1* as ectoderm markers (fig. 6F). N-ntES cells and TT2 ES cells were injected separately into the flanks of nude mice to monitor the devel-

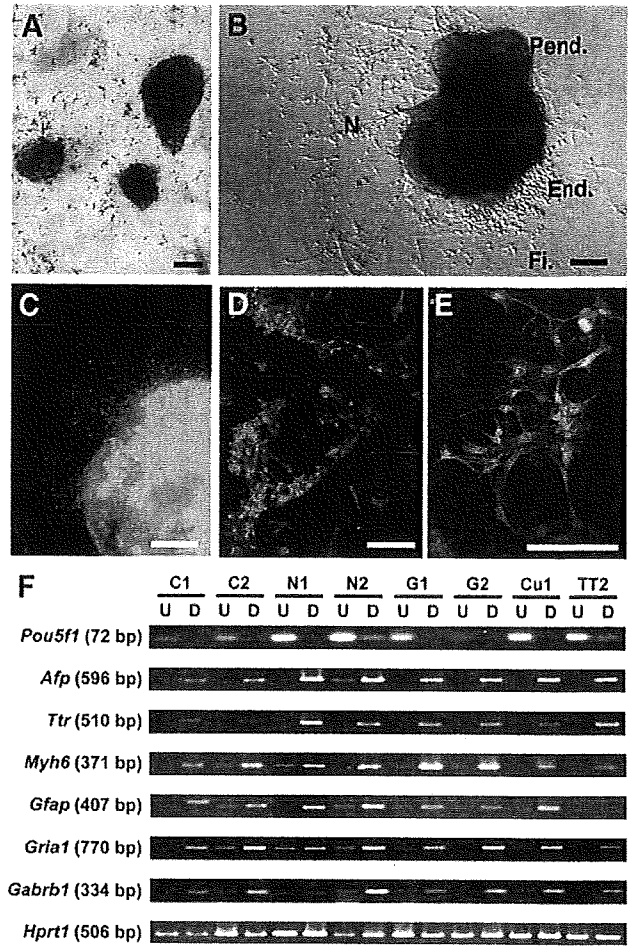

Fig. 6. Differentiation of ES cells derived from neuronal cell nuclei in vitro. **A** Alkaline phosphatase activity was detected in ES cell colonies (brown) but not in feeder cells. **B** Gross morphology of the Cam-1 ES cells differentiated in vitro. A variety of cell types was observed, including neuronal (N, ectoderm), fibroblast-like (Fi, mesoderm), endothelial-like (End., endoderm) and parietal endoderm-like (Pend.) cells. **C–E** Neuronal induction of the ES cells in vitro by retinoic acid. Permanent genetic marking was achieved by GFP expression in the Cam-1 (**C**, **D**) and Cam-2 (**E**) lines. Indirect immunofluorescence revealed neuronal ectodermal derivatives stained with antibodies to GAD67 (**C**) and NeuN (**D**), and mesodermal mesenchymal cells reactive to the anti-desmin antibody (**E**). Scale bars = 50 μm. **F** RT-PCR analyses of marker gene expressions in undifferentiated (U) ES cells and differentiated (D) EB cells. The ES cells were cultured for 3 days on feeder cells with LIF, and the EB cells for 8 days without feeder cells or LIF.

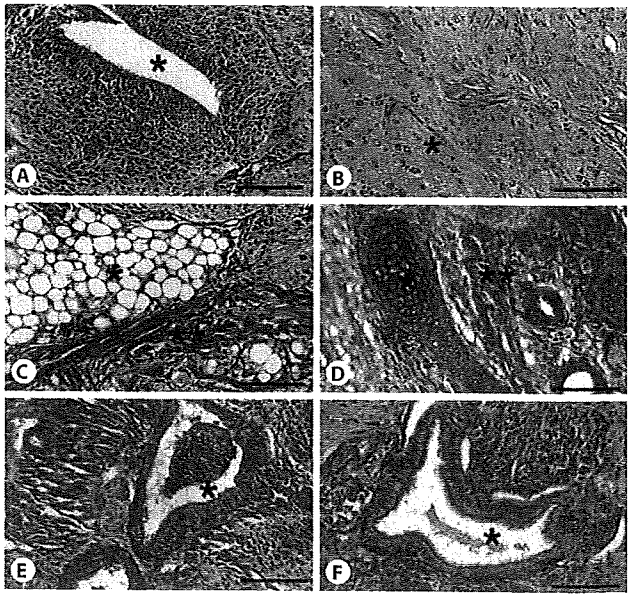

Fig. 7. NtES cell differentiation in vivo. Histological examination by means of hematoxylin and eosin staining (**A**, **C**, **E**) and staining with the antibody to GAD67 of teratocarcinomas resulting from Cam-2 injection (**B**, **D**, **F**). Sections show the presence of ectoderm, i.e., neural epithelium (asterisks in **A**, **B**), mesoderm, i.e., fatty tissue (single asterisk in **C**), cartilage (single asterisk in **D**), and muscle (double asterisks in **C**, **D**), and endoderm, i.e., ciliated epithelium (asterisks in **E**, **F**). Bars = 100 μm.

opment of teratocarcinomas in vivo. 3–5 weeks after the injections, with the exception of Nex-2, all ntES cells and the TT2 ES cells had given rise to tumors. Histological examination showed that the teratocarcinomas from each ES cell were composed of all 3 embryonic germ layers; that is, neural epithelium (ectoderm), muscle and cartilage (mesoderm), and the ciliated epithelium (endoderm) (fig. 7A–F).

Discussion

We previously described our use of NT to study the chromosomal constitution of the nuclei from postmitotic neurons [Osada et al., 2002]. Our findings were consistent with the observation of chromosomal variations in the developing and adult brain [Rehen et al., 2002]. However, since the detection of any genetic changes in the nervous system is currently technically challenging [Chun, 2004], we need more accurate methods for the assessment of the chromosomal properties of neurons. To achieve this objective, in the present study we analyzed the chromosomes of neuron-injected NT embryos at 3 developmental stages (fig. 1).

The SKY method was used to detect balanced and unbalanced chromosomal translocations in metaphase spreads as well as to determine more accurately the number of chromosomes that were gained or lost than can be attained with conventional G-banding in the mouse. First, we examined the chromosomal constitution of N-ntES cells, which were presumably derived from single N-NT embryos, and found chromosomal rearrangements in all Nex-2 N-ntES cells examined. These N-ntES cells with translocations did not form tumors, although in vitro differentiation revealed the expression of several differentiation marker genes in the Nex-2-derived EB cells. We therefore speculate that the translocation may have a suppressive effect on tumorigenesis in vivo.

Determination of whether ntES cells are established from embryos with aneuploidy, which has been reported to occur in neural subpopulations, is of interest [Rehen et al., 2001; Kingsbury et al., 2005]. It is also important to establish whether the chromosomal rearrangements in the N-ntES cells reflect genomic changes that normally occur in the nervous system, or if they are de novo mutations generated during the experimental protocol. We observed that only a minor subpopulation of the N-ntES cells possessed chromosomal rearrangements, suggesting that the karyotypic changes were generated during the experimental processes. We further analyzed the chromosomal constitution of the N-NT embryos in the earlier developmental stages. First, we re-examined the chromosome spreads of the N-NT and C-NT embryos during the first mitotic cleavage. Aneuploidy was detected in the mitotic spreads from N-NT and C-NT embryos, but no specific aneuploid chromosomes were observed. Moreover, the difference in the frequency of aneuploidy between the N-NT and C-NT embryos during the first mitotic cleavage was not statistically significant.

The SKY analyses yielded other cytogenetic information, including findings related to translocation events. Both balanced and unbalanced translocations were detected in the N-NT embryos. Since the translocation patterns were diverse, it was not clear whether the chromosomal changes were innately generated in the donor cell nuclei. To examine this issue further, we assessed premature chromosome condensation (PCC) figures, which form within 2–3 h after injection of exogenous DNA into the ooplasm. We detected aneuploidy, fragmented chromatids, and undercondensed chromatids, which were also detected during the first mitotic cleavage in our previous study [Osada et al., 2002]. DNA damage may lead to inappropriate chromatid condensation in the ooplasm because a lack of DNA repair enzymes can induce aberrant condensation of chromosomes at metaphase [Hittelman et al., 1974; Deckbar et al., 2007].

The causes of translocation in the condensed chromatids in neuron-injected oocytes are largely unknown. One possibility is that the translocation is innately generated in the donor nucleus. Such a translocation would change the global nuclear architecture of the neuronal genome, which may then define the gene expression profiles that support neuronal functions. However, no evidence of DNA recombination in the nervous system has been found so far. Another possibility is that instability of the chromosomes in ES cells [Humpherys et al., 2001] results in translocation. The translocations detected in our study may have been generated during the transformation into ES cells. However, the translocations observed in the NT embryos, especially in the condensed chromatids of the NT oocytes, could not have resulted from such an event.

Another possibility is that the DNA repair machinery in the ooplasm is activated when the neuronal DNA is exposed to the oocyte cytoplasm. DNA repair-associated proteins are expressed and function in oocytes [Ashwood-Smith and Edwards, 1996; Kuznetzov et al., 2007], and evidence has been presented that mutations occur in neuronal DNA in association with aging [Lu et al., 2004; Gonitel et al., 2008]. It is possible that double-strand

breaks (DSBs) in the neuronal DNA can be repaired in oocytes within a short period of time as a result of non-homologous end joining. In this case, translocation would occur in non-specific DNA sequences, many of which would have no apparent effect on cell differentiation or physiology. However, our data revealed defects in the differentiation potentials of the NT-ES cells (Nex-2) in vivo that exhibited clonally balanced translocations. In addition, it has been shown recently that DSBs in DNA mediated by topoisomerase II are generated at transcriptionally active loci [Ju et al., 2006], while we found that the BAC clone RP23-330K23 spanned the 6q breakpoint of T(1;6) in the Nex-2 NT-ES cells. Since the entire region of the BAC clone RP23-330K23 is contained within the *Fam19a1* gene, the 6q breakpoint of T(1;6) was also mapped within the *Fam19a1* gene. The function of the *Fam19a1* gene product is not known but its expression is restricted to the brain [Tom Tang et al., 2006]. We speculate that the observed chromosomal translocation in the Nex-2 NT-ES cells occurred at a gene locus where dsDNA break-mediated transcription was actively taking place.

Previous studies have demonstrated that chromosomal breaks, observed as the fragmentation of chromosomes, may be a cause of the developmental inefficacy of NT-embryos [Wakayama et al., 2000]. The SKY analysis we used in the present study enabled us to visualize unbalanced and balanced chromosomal translocations and to identify the chromosomal alterations. Although our data showed that aneuploid or fragmented chromosomes were more common, translocations in the DNA of the N-NT embryos were also detected. Since we did not detect translocations in the C-NT DNA, such changes may be specific for N-NT embryos, not for NT embryos in general, and are therefore possibly responsible for the observed inefficient developmental rate of the N-NT embryos [Osada et al., 2005].

To summarize, we examined the chromosomal constitution of oocytes injected with DNA from postmitotic neurons and their derivative ntES cells. Translocations were detected in the ntES cells derived from N-NT embryos and in the NT embryos during PCC formation and the first mitotic cleavage. Our findings indicate that some donor neurons may exhibit chromosomal changes that restrict the developmental potential of the neuronal genome. We also detected frequent chromosomal changes during the first cleavage of N-NT embryos. These findings raise the possibility that DNA repair systems activated in the ooplasm may cause accidental chromosomal rearrangements. Although the ontology of the chromosomal rearrangements in N-NT oocytes is still unclear, our data provide new evidence for the genetic/epigenetic regulation of neuronal genomes through a unique biological window.

Somatic reprogramming can currently be achieved by means of induced pluripotent stem (iPS) cell technology [Takahashi et al., 2006]. The creation of a massive collection of neuron-derived monoclonal cell lines as a source for abundant DNA from individual neurons would create a valuable resource for investigators in this field. Since the re-entry of neurons into the cell cycle causes apoptosis in neurodegenerative diseases [Kruman et al., 2004], the data from genetic studies of neuronal DNA may reveal ways to protect neurons from degeneration, in particular by clarifying which reprogramming factors regulate the ability of postmitotic neurons to proliferate. In combination with high-performance sequencing technology [Eid et al., 2009], single neuron-based whole-genome sequencing can be expected to provide definitive evidence for genetic contributions to the complexity and specificity of individual neurons.

Acknowledgements

We thank Mr. Jan K. Visscher for proofreading and editing of the manuscript and Dr. Hirokazu Kusakabe for informative insight into cytogenetic analyses of early embryos.

This study was supported in part by grant-in-aid from the Ministry of Education, Science, Sports, and Culture of Japan (T.O., N.K., and T.Y.), the CREST (Core Research for Evolutional Science and Technology) of JST (Japan Science and Technology Agency) (Y.T.), and a COE (Center of Excellence) funding program of Osaka University (T.O.).

References

Albert B, Johnson A, Lewis J, Raff M, Roberts K, Walter P (eds): Cancer, in: Molecular Biology of the Cell, 4th ed, pp 1187–1216 (Garland Science, New York 2002).

Ashwood-Smith MJ, Edwards RG: DNA repair by oocytes. Mol Hum Reprod 2:46–51 (1996).

Bain G, Kitchens D, Yao M, Huettner JE, Gottlieb DI: Embryonic stem cells express neuronal properties in vitro. Dev Biol 168:342–357 (1995).

Chun J: Choice, choice, choice. Nat Neurosci 7: 323–325 (2004).

Chun JJ, Schatz DG, Oettinger MA, Jaenisch R, Baltimore D: The recombination activating gene-1 (RAG-1) transcript is present in the murine central nervous system. Cell 64:189–200 (1991).

Deckbar D, Birrauz J, Krempler A, Tchouandong L, Beucher A, et al: Chromosome breakage after G2 checkpoint release. J Cell Biol 176: 749–755 (2007).

Eid J, Fehr A, Gray J, Luong K, Lyle J, et al: Real-time DNA sequencing from single polymerase molecules. Science 323:133–138 (2009).
Gonitel R, Moffitt H, Sathasivam K, Woodman B, Detloff PJ, et al: DNA instability in post-mitotic neurons. Proc Natl Acad Sci USA 105:3467–3472 (2008).
Gossen JA, de Leeuw WJ, Tan CH, Zwarthoff EC, Berends F, et al: Efficient rescue of integrated shuttle vectors from transgenic mice: a model for studying mutations in vivo. Proc Natl Acad Sci USA 86:7971–7975 (1989).
Hittelman WN, Rao PN: Premature chromosome condensation. I. Visualization of x-ray-induced chromosome damage in interphase cells. Mutat Res 23:251–158 (1974).
Hogan B, Beddington R, Constantini F, Lacy E (eds): Isolation, culture, and manipulation of embryonic stem cells, in: Manipulating the Mouse Embryo; a Laboratory Manual, 2nd ed, pp 253–290 (Cold Spring Harbor Press, New York 1994).
Humpherys D, Eggan K, Akutsu H, Hochedlinger K, Rideout WM 3rd, et al: Epigenetic instability in ES cells and cloned mice. Science 293:95–97 (2001).
Johnson FB, Sinclair DA, Guarente L: Molecular biology of aging. Cell 96:291–302 (1999).
Ju BG, Lunyak VV, Perissi V, Garcia-Bassets I, Rose DW, et al: A topoisomerase IIbeta-mediated dsDNA break required for regulated transcription. Science 312:1798–1802 (2006).
Kakazu N, Taniwaki M, Horiike S, Nishida K, Tatekawa T, et al: Combined spectral karyotyping and DAPI banding analysis of chromosome abnormalities in myelodysplastic syndrome. Genes Chromosomes Cancer 26: 336–345 (1999).
Kingsbury MA, Friedman B, McConnell MJ, Rehen SK, Yang AH, et al: Aneuploid neurons are functionally active and integrated into brain circuitry. Proc Natl Acad Sci USA 102: 6143–6147 (2005).
Kruman II, Wersto RP, Cardozo-Pelaez F, Smilenov L, Chan SL, et al: Cell cycle activation linked to neuronal cell death initiated by DNA damage. Neuron 41:549–561 (2004).
Kuznetzov S, Pellegrini M, Shuda K, Fernandez-Capetillo O, Liu Y, et al: RAD51C deficiency in mice results in early prophase I arrest in males and sister chromatid separation at metaphase II in females. J Cell Biol 176:581–592 (2007).
Lee JD, Kamiguchi Y, Yanagimachi R: Analysis of chromosome constitution of human spermatozoa with normal and aberrant head morphologies after injection into mouse oocytes. Hum Reprod 9:1941–1946 (1996).
Liyanage M, Coleman A, du Manoir S, Veldman T, McCormack S, et al: Multicolour spectral karyotyping of mouse chromosomes. Nat Genet 14:312–315 (1996).
Lu T, Pan Y, Kao SY, Li C, Kohane I, et al: Gene regulation and DNA damage in the aging human brain. Nature 429:883–891 (2004).
Mattick JS, Mehler MF: RNA editing, DNA recoding and the evolution of human cognition. Trends Neurosci 31:227–233 (2008).
Mikamo K, Kamiguchi Y: A new assessment system for chromosomal mutagenicity using oocytes and early zygotes of the Chinese hamster, in Ishihara T, Sasaki MS (eds): Radiation-Induced Chromosome Damage in Man, pp 411–432 (Alan R. Liss, New York 1983).
Muotri AR, Chu VT, Marchetto MC, Deng W, Moran JV, Gage FH: Somatic mosaicism in neuronal precursor cells mediated by L1 retrotransposition. Nature 435:903–910 (2005).
Osada T, Kusakabe H, Akutsu H, Yagi T, Yanagimachi R: Adult murine neurons: their chromatin and chromosome changes and failure to support embryonic development as revealed by nuclear transfer. Cytogenet Genome Res 97:7–12 (2002).
Osada T, Tamamaki N, Song SY, Kakazu N, Yamazaki Y, et al: Developmental pluripotency of the nuclei of neurons in the cerebral cortex of juvenile mice. J Neurosci 25:8368–8374 (2005).
Redon R, Ishikawa S, Fitch KR, Feuk L, Perry GH, et al: Global variation in copy number in the human genome. Nature 444:444–454 (2006).
Rehen SK, McConnell MJ, Kaushal D, Kingsbury MA, Yang AH, Chun J: Chromosomal variation in neurons of the developing and adult mammalian nervous system. Proc Natl Acad Sci USA 98:13361–13366 (2001).
Rudak E, Jacob PA, Yanagimachi R: Direct analysis of the chromosome constitution of human spermatozoa. Nature 274:911–913 (1978).
Takahashi K, Tanabe K, Ohnuki M, Narita M, Ichisaka T, et al: Induction of pluripotent stem cells from adult human fibroblasts by defined factors. Cell 131:861–872 (2006).
Tom Tang Y, Emtage P, Funk WD, Arterburn M, Park EE, Rupp F: TAFA: a novel secreted family with conserved cysteine residues and restricted expression in the brain. Genomics 83:727–734 (2006).
Wakayama T, Tateno H, Mombaerts P, Yanagimachi R: Nuclear transfer into mouse zygotes. Nat Genet 24:108–109 (2000).
Yagi T, Tokunaga T, Furuta Y, Nada S, Yoshida M, et al: A novel ES cell line, TT2, with high germline-differentiating potency. Anal Biochem 214:70–76 (1993).
Ziegler D, Masui Y: Control of chromosome behavior in amphibian oocytes. I. The activity of maturing oocytes including chromosome condensation in transplanted brain nuclei. Dev Biol 35:283–292 (1973).

再生医学

マイクロアレイとNIA array analysisを用いた心筋分化誘導因子の探索

Exploration of the cardiomyogenic differentiation factor using DNA micro array and NIA array analysis

マイクロアレイを用いた心筋分化誘導因子の探索

近年の研究から心筋細胞の発生過程において，骨形成因子(bone morphogenetic protein：Bmp)や線維芽細胞増殖因子(fibroblast growth factor：Fgf)などのサイトカインによって誘導されるCsx/Nkx2.5やGata4，Mef2cのような転写因子は，その心筋細胞の運命決定因子として重要な役割を担っている[1]．このような数多くの心筋細胞の発生に関与する主要な転写因子群の機能は明らかになりつつあるものの，心筋分化誘導のマスタージーンは確認されていない．これは心筋細胞の発生には複数の遺伝子が経時的に関与するため，あるいはこれらの転写因子群の機能を制御している別の因子が存在しているためであると考えられている．このような背景から心筋分化に関連する遺伝子の選択のために，マイクロアレイを用いた網羅的な遺伝子発現解析が行われてきた．しかし，複数の細胞のマイクロアレイの結果をもとに特定の遺伝子を選択することは非常に困難である．そのため，統計解析を用いた特定の細胞群特異的な発現を示す遺伝子を選択する手法が必要となる．

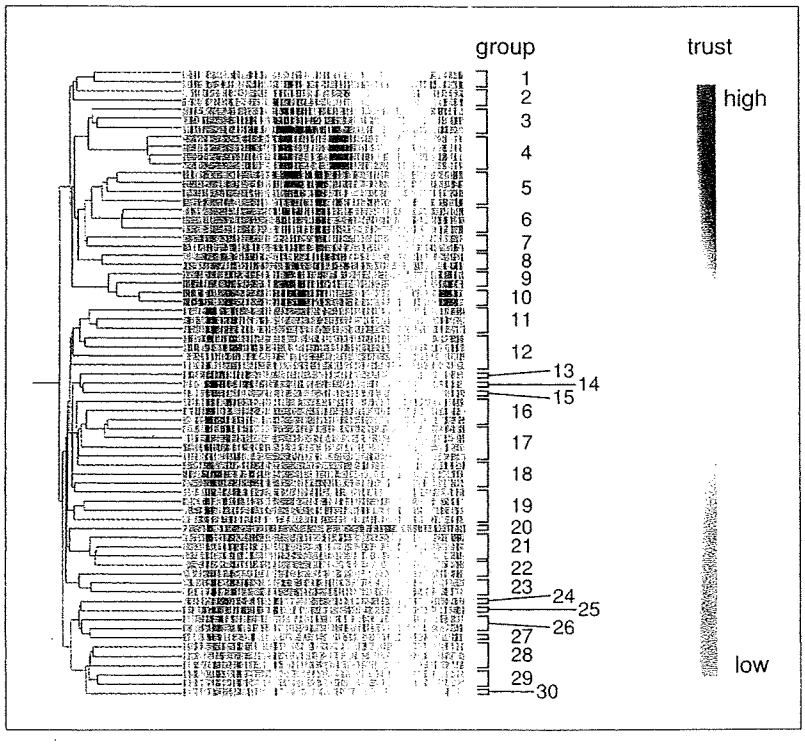

図1　69種類の培養ヒト細胞の遺伝子発現解析

GeneSpring softwareを用いた69種類のヒト細胞の遺伝子発現解析結果．発現データの近似している細胞をグループ化したところ，30グループにまとめることができた．

NIA array analysisによる心筋分化誘導因子の選択と今後の展望

これまで著者らのチームは，月経血や胎盤などの初代培養細胞とマウス胎児心筋細胞の共培養による心筋分化誘導に成功してきた[2-4]．この知見をもとに，これら心筋分化しやすい細胞と分化しにくい細胞のマイクロアレイデータ，ならびにヒト胚性幹細胞などのマイクロアレイデータ(NCBI Gene Expression Omnibusデータベースから取得)の合計69種類のデータを用い，GeneSpring GX softwareにて遺伝子発現を比較した．さらに，近似した遺伝子発現データを示す細胞を任意にグループ化したところ，30グループに区分できた(図1)．この30グループのうち21グループは，共培養法

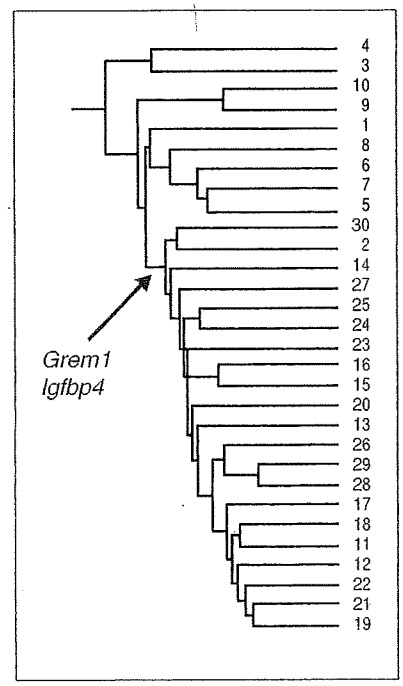

図2　培養ヒト細胞の階層的クラスタ分析

図1でまとめられた30グループに対してNIA array analysisを用いた階層的クラスタ分析の結果．このとき，心筋分化が可能な細胞群(21グループ；赤字)特異的な遺伝子として*Grem1*と*Igfbp4*を選択できた．

や胚体形成によって心筋細胞に分化誘導が可能な細胞グループであった．そこで，この21グループ特異的な遺伝子を同定するために，マイクロアレイの結果を簡便に統計解析処理できるwebアプリケーションNIA array analysis (http:/ /lgsun.grc.nia.nih.gov/ANOVA/)[5]を用いて階層的クラスタ分析を行った．この結果，この21グループ特異的遺伝子として，2つの心筋分化誘導候補遺伝子(*Grem1*, *Igfbp4*)を選択できた(図2)．この2遺伝子の心筋分化誘導能を検証したところ，Bmpアンタゴニストである Grem1 は分化誘導初期の Bmp シグナルを阻害することで[6]，Igfbp4 は分化誘導後期の canonical Wnt/β-catenin シグナルを阻害することで[7]，胚性細胞の心筋分化を促進していることが明らかになった．

これらの結果から本手法は心筋細胞のみならず，何らかの特徴的な性質をもつ細胞群のマイクロアレイデータを用いることで，臓器特異的な分化誘導因子や，近年注目されているクロマチンリモデリング因子の探索に役立つ可能性がある．さらに，NCBI Gene Expression Omnibus にアップロードされているデータも利用できるため，*in silico* での解析や考察の確認にも有用である．今後はこれらの手法を組み合わせ，あらたな心筋分化誘導因子の探索とその評価解析も同時に行っていく．

1) Shiojima, I. and Komuro, I.：Cardiac developmental biology：from flies to humans. *Jpn J. Physiol.*, **55**：245-254, 2005.
2) Okamoto, K. et al.：Working' cardiomyocytes exhibiting plateau action potentials from human placenta-derived extraembryonic mesodermal cells. *Exp. Cell Res.*, **313**：2550-2562, 2007.
3) Hida, N. et al.：Novel cardiac precursor-like cells from human menstrual blood-derived mesenchymal cells. *Stem Cells*, **26**：1695-1704, 2008.
4) Nishiyama, N. et al.：The significant cardiomyogenic potential of human umbilical cord blood-derived mesenchymal stem cells *in vitro*. *Stem Cells*, **25**：2017-2024, 2007.
5) Sharov, A. A. et al.：A web-based tool for principal component and significance analysis of microarray data. *Bioinformatics*, **21**：2548-2549, 2005.
6) Kami, D. et al.：Gremlin enhances the determined path to cardiomyogenesis. *PLoS ONE*, **3**：e2407, 2008.
7) Zhu, W. et al.：IGFBP-4 is an inhibitor of canonical Wnt signalling required for cardiogenesis. *Nature*, **454**：345-349, 2008.

上　大介，石井隆雅，梅澤明弘，渡邉昌俊／ Daisuke KAMI[1], Ryuga ISHII[3], Akihiro UMEZAWA[3] and Masatoshi WATANABE[2]

横浜国立大学情報通信による医工融合イノベーション創生グローバルCOE[1]，同大学院工学研究院機能の創生部門過程の機能と安全分野[2]，国立成育医療センター研究所生殖医療研究部[3]

糖尿病・内分泌代謝学

劇症1型糖尿病――最新動向

Recent progress in fulminant type 1 diabetes

劇症1型糖尿病とは

劇症1型糖尿病は2000年に報告された“非常に急速でほぼ完全な膵β細胞破壊の結果生じる糖尿病”と定義される糖尿病のサブタイプである[1]．日本人急性発症1型糖尿病の約20%を占め，GAD抗体などの膵島関連自己抗体がおおむね陰性であることが特徴であり，他の80%に相当する自己免疫性1型糖尿病と対照的である．そのほかに，ケトアシドーシスを伴って非常に急激に発症することや発症時に著明な高血糖を認めるにもかかわらず，HbA_{1c}は正常または軽度上昇にとどまる，といった臨床的な特徴も明らかになっている．

劇症1型糖尿病発症に関与する遺伝因子として，HLA(human leukocyte antigen)遺伝子が知られていた．すなわち，class II HLA のDR-DQハプロタイプのなかで，劇症1型糖尿病ではDR4-DQ4の頻度が高く，とくにこのハプロタイプをホモで有する場合のオッズ比は13.3と，非常に高い値を示すことが報告されていた．ちなみに，DR4-DQ4は通常 *DRB1*0405-DQB1*0401* という遺伝子型によりコードされる．

劇症1型糖尿病とCTLA-4

今回HLAに加えて，やはり免疫反応に関与する分子であるCTLA-4(cytotoxic T lymphocyte antigen-4)遺伝子と劇症1型糖尿病との関連が明らかにされた．

CTLA-4は抗原提示細胞(マクロファージや樹状細胞)上に発現する分子で，T細胞のB7-1(CD80)

表1　CTLA-4遺伝子多型(文献[2]より作成)

	+49GG	CT60AA
劇症1型(n=55)		
オッズ比(95%CI)		2.68(1.13～6.37)
p value	NS	0.021
急性発症1A型(n=90)		
オッズ比(95%CI)	2.26(1.41～3.60)	
p value	0.0005	NS

はじめに
Introduction

渡邉昌俊
Masatoshi WATANABE
横浜国立大学大学院工学研究院機能の創生部門過程の機能と安全分野（医工学）

ナノテクノロジーの発展はすさまじく，いろいろな分野への応用が期待されている．当然のことながら医学と工学の連携で，drug delivery system（DDS）や分子イメージングなど医療への応用が図られている．

ナノ粒子メディスンという言葉は，ナノテクノロジーのなかで重要な技術・素材であるナノ粒子と医療を合わせた造語である．ナノ粒子はバルクと異なり，活性度と反応性が飛躍的に高まり，その特性である電磁気的・光学的・機械的性質などが大きく変わることが知られている．本特集では，このナノ粒子の再生から癌治療にわたる医療への応用を中心に組ませていただいた．

一方，ナノテクノロジーのリスク，とくにナノマテリアルの細胞毒性が問題となっているが，その生体への影響について十分な知見は得られていない．本年（2009）3月には厚生労働省より“ナノマテリアルに対するばく露防止等のための予防的対応について”（通知）がだされた．このような状況で，多層カーボンナノチューブによる実験動物での中皮腫の発生に関して異なる報告がだされている[1]．著者自身，病理学者として，重要な科学技術であるナノマテリアルの細胞毒性に十分注意を払いつつ，評価し使用していく必要があると考える．また，ナノ粒子が原因不明の肉芽種の原因であるという説も出ており，病因論的には非常に興味深い．

本特集号では，2007年の化学工学会第39会秋期大会シンポジウム（マイクロプロセスからみた細胞・組織工学の展開），2008年の異分野融合ナノテクノロジー横浜コロキウム，2008年の第55回日本臨床検査医学会学術集会シンポジウム（医学領域におけるナノ粒子展開をめぐる話題）などで講演を行っていただいた研究者に執筆をお願いした．この特集を読まれてナノ粒子をめぐる問題を理解していただき，ナノ粒子を含むナノテクノロジーを用いた医療のさらなる発展に力となれば幸いである．

1) Sakamoto, Y. et al.：Induction of mesothelioma by a single intrascrotal administration of multi-wall carbon nanotube in intact male Fischer 344 rats. *J. Toxicol. Sci.*, **34**：65-76, 2009.